25. I. Mahadevan and M. Rasmussen, *Tetrahedron*, 1993, **49**, 7337-7352.
26. See, for example, A. L. J. Beckwith and A. A. Zavitsas, *J. Am. Chem. Soc.*, 1995, **117**, 607-614.
27. L. Strekowski, M. Hojjat, S. E. Patterson, and A. S. Kiselyov, *J. Heterocycl. Chem.*, 1994, **31**, 1413-1416.
28. F. Neumann and K. Jug, *J. Org. Chem.*, 1994, **59**, 6442-6447.
29. T. S. Stevens, *J. Chem. Soc.*, 1930, 2107-2119.
30. A. Campbell, A. H. J. Houston, and J. Kenyon, *J. Chem. Soc.*, 1947, 93-95.
31. G. Wittig, R. Mangold, and G. Felletschin, *Liebigs Ann. Chem.*, 1948, **560**, 116-127.
32. C. R. Hauser and S. W. Kantor, *J. Am. Chem. Soc.*, 1951, **73**, 1437-1441.
33. R. W. Jemison and D. G. Morris, *J. Chem. Soc., Chem. Commun.*, 1969, 1226-1227.
34. M. J. S. Dewar and C. A. Ramsden, *J. Chem. Soc., Perkin Trans. 1*, 1974, 1839-1844.
35. W. D. Ollis, M. Rey, I. O. Sutherland, and G. L. Closs, *J. Chem. Soc., Chem. Commun.*, 1975, 543-545.
36. U. H. Dolling, G. L. Closs, A. H. Cohen, and W. D. Ollis, *J. Chem. Soc., Chem. Commun.*, 1975, 545-547.
37. A. P. Stamegna and W. E. McEwen, *J. Org. Chem.*, 1981, **46**, 1653-1655.
38. W. D. Ollis, M. Rey, and I. O. Sutherland, *J. Chem. Soc., Perkin. Trans. 1*, 1983, 1009-1027.
39. G. L. Heard and B. F. Yates, *Aust. J. Chem.*, 1994, **47**, 1685-1694.
40. G. L. Heard and B. F. Yates, *J. Mol. Struct. (Theochem)*, 1994, **310**, 197-204.
41. T. S. Stevens, E. M. Creighton, A. B. Gordon, and M. MacNicol, *J. Chem. Soc.*, 1928, 3193-3197.
42. S. Pine, *J. Chem. Educ.*, 1971, **48**, 99-102.
43. G. L. Heard and B. F. Yates, *J. Comput. Chem.*, 1996, **17**, 1444-1452.
44. G. L. Heard, T. D. Wale, and B. F. Yates, unpublished work.
45. G. J. Tarrant, J. B. Bremner, and B. F. Yates, unpublished work.
46. T. S. Bailey, PhD thesis, University of Tasmania, 1995.
47. N. Shirai, Y. Watanabe, and Y. Sato, *J. Org. Chem.*, 1990, **55**, 2767-2770.
48. T. Tanaka, N. Shirai, J. Sugimori, and Y. Sato, *J. Org. Chem.*, 1992, **57**, 5034-5036.
49. T. Usami, N. Shirai, and Y. Sato, *J. Org. Chem.*, 1992, **57**, 5419-5425.
50. T. Kitano, N. Shirai, M. Motoi, and Y. Sato, *J. Chem. Soc., Perkin Trans. 1*, 1992, 2851-2854.
51. Y. Sato, N. Shirai, Y. Machida, E. Ito, T. Yasui, Y. Kurono, and K. Hatano, *J. Org. Chem.*, 1992, **57**, 6711-6716.
52. A. Sakuragi, N. Shirai, Y. Sato, Y. Kurono, and K. Hatano, *J. Org. Chem.*, 1994, **59**, 148-153.
53. Y. Sato and N. Shirai, *J. Pharm. Soc. Jpn.*, 1994, **114**, 880-887.
54. G. L. Heard and B. F. Yates, *J. Org. Chem.*, 1996, **61**, 7276-7284.
55. T. Tanzawa, M. Ichioka, N. Shirai, and Y. Sato, *J. Chem. Soc., Perkin Trans. 1*, 1995, 431-435.
56. Y. Hayashi and R. Oda, *Tetrahedron Lett.*, 1968, 5381-5384.
57. A. P. Marchand, K. C. V. Ramanaiah, S. G. Bott, J. C. Gilbert, and S. Kirschner, *Tetrahedron Lett.*, 1996, **37**, 8101-8104.
58. R. T. Kroemer, H. Gstach, K. R. Liedl, and B. M. Rode, *J. Chem. Soc., Perkin Trans. 2*, 1994, 2129-2135; M. T. Nguyen, G. Raspoet, and L. G. Vanquickenborne, *J. Chem. Soc., Perkin Trans. 2*, 1995, 1791-1795.
59. As an example of a potential energy surface study involving a model heterocyclic ligand, see K. E. Frankcombe, K. J. Cavell, R. B. Knott, and B. F. Yates, *J. Chem. Soc., Chem. Commun.*, 1996, 781-782.

Reaction Path Following

H. Bernhard Schlegel

Wayne State University, Detroit, MI, USA

Abbreviations

CLQA = corrected local quadratic approximation; DDRP = dynamically defined reaction path; DRP = dynamic reaction path; ES = Euler stabilization method; GS = Gonzalez and Schlegel method; IMK = Ishida-Morokuma-Kormornicki method; LQA = local quadratic approximation; MB = Müllar-Brown method; MEP = minimum energy path; ODE = ordinary differential equations; SDRP = steepest descent reaction path; VRI = valley-ridge inflection.

1 INTRODUCTION

A reaction path is a pathway across a potential energy surface connecting reactants and products. A potential energy surface describes the changes in the energy of a molecular system as its structure is varied. In constructing a potential energy surface, one invokes the *Born-Oppenheimer approximation* to separate the motion of the atoms or nuclei from motion of the electrons. For two degrees of freedom, a potential energy surface can be visualized as a hilly landscape. As illustrated in Figure 1, the reactants and products are valleys on the surface, and are separated from each other by ridges and mountain ranges. A reaction is represented by motion across the potential energy surface from the reactant valley, over a mountain pass to the product valley, possibly through additional valleys representing reactive intermediates. This pathway describes the mechanism of the reaction, and can also be used to calculate the reaction rate by variational transition state theory (see ***Transition State Theory***). Reaction paths have been the subject of some recent reviews.[1-4] This article discusses a number of methods for calculating reaction paths.

Of all the paths across a potential energy surface, consider the one that requires the least increase in energy to get from reactants to products. The transition structure is the highest energy point on this lowest energy reaction path, and can be found by various geometry *optimization* techniques (see ***Geometry Optimization: 1*** and ***Geometry Optimization: 2***). Most methods for calculating reaction paths start from the transition state and go downhill. It is difficult to define an appropriate uphill path beginning with the reactants or products, since all directions are uphill. The shallowest ascent path can be defined (see gradient extremals,[5] discussed below), but will not necessarily reach the desired transition structure, or even the lowest energy transition structure. A steepest descent reaction path (SDRP) from the transition structure to reactants

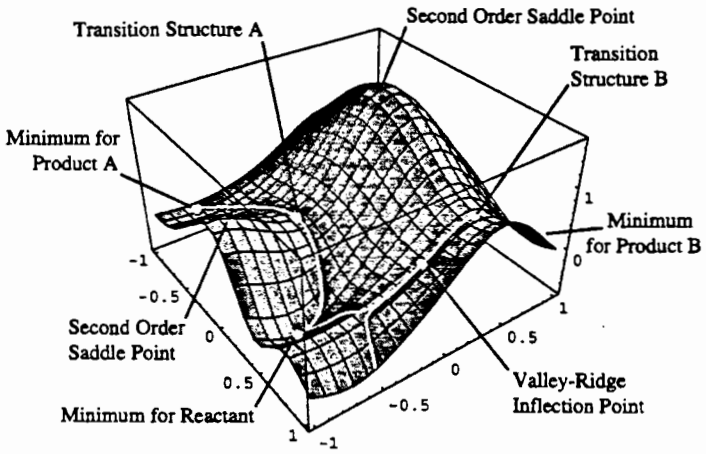

Figure 1 A model potential energy surface illustrating minima, transition states, reaction paths and a valley-ridge inflection point. Reproduced with permission from H. B. Schlegel, in 'Modern Electronic Structure Theory', ed. D. R. Yarkony. Copyright (1995) World Scientific Publishing

and to products is unique in a given coordinate system; it is also termed the minimum energy path (MEP) and is usually identified as the reaction path for the system. Figure 1 shows a steepest descent reaction path on model surface. The steepest descent reaction path can be followed in Cartesian coordinates or any of a variety of internal coordinates, but each of these paths is somewhat different since the steepest descent direction depends upon the coordinate system. One coordinate system has special significance from a dynamical point of view. In mass-weighted Cartesian coordinates, the steepest descent step is in the direction that a stationary molecule (i.e., without kinetic energy) would be accelerated by classical mechanics. The steepest descent reaction path in mass-weighted Cartesian coordinates is also known as the intrinsic reaction coordinate (IRC).[6] The same IRC can also be generated by following the path in internal coordinates, provided that the appropriate mass weighting is used.[7]

Steepest descent reaction paths are not the same as classical trajectories on potential energy surfaces. Classical trajectories have nonzero kinetic energy and can deviate quite widely from the steepest descent path. However, if a trajectory were started at the transition structure heading along the transition vector and all the kinetic energy were continuously removed, the result would be an IRC. A dynamic reaction path (DRP)[8] is a trajectory with kinetic energy added to one or more degrees of freedom of the molecule, and can give some indication of the dynamic effects in a reaction. The accurate simulation of reaction rates and molecular dynamics requires the calculation of many trajectories with appropriate sampling of initial conditions to get statistically significant results (see ***Scaled Particle Theory*** and ***Trajectory Simulations of Molecular Collisions: Classical Treatment***). Although some trajectory calculations can be computed directly from quantum mechanical potential calculations,[9] most classical trajectory studies are carried out on analytical functions fitted to energy surfaces. Since global fits to potential energy surfaces are difficult to obtain, simpler methods for calculating rates from more limited data about the surface are desirable. Statistical mechanical approaches for reaction rates such as variational transition state theory and reaction path Hamiltonian methods (see ***Reaction Path Hamiltonian and its Use for Investigating Reaction Mechanisms*** and ***Transition State Theory***) require only local information about the energy surface along the reaction path. Thus, reaction path following methods are important for reaction rate calculations as well as for determining reaction mechanisms.

If a reaction path must be started from a minimum, then a unique uphill direction needs to be chosen. A shallowest ascent path can be defined as a series of uphill steps, such that the magnitude of the first derivative vector, or gradient, is always a minimum (an extremum) along a constant energy contour. This path is also called a gradient extremal.[5] At any point along a gradient extremal, the gradient is an eigenvector of the second derivative matrix or Hessian (see *Hessian Matrix*). Since a gradient extremal path is defined using local properties of the potential energy surface (gradient and Hessian), one can

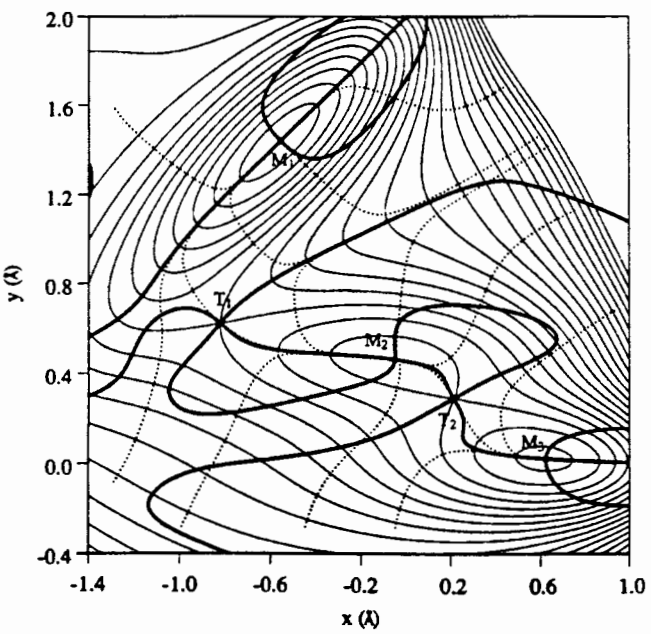

Figure 2 Gradient extremal paths on the Müller-Brown model potential energy surface. Solid lines: contours; dotted lines: selected steepest descent lines; bold lines: gradient extremals. Reproduced with permission from J. Q. Sun and K. Ruedenberg, *J. Chem. Phys.*, 1993, **98**, 9707. Copyright (1993) American Institute of Physics

readily check if a point is on the path. By contrast, the only way to determine if a point is on a steepest descent reaction path is to follow the path from the transition structure. The main drawback of gradient extremal paths is that they tend to wander about the potential energy surface, as shown in Figure 2, without necessarily following the same valleys as the steepest descent reaction paths. Furthermore, gradient extremals branch or bifurcate more frequently than steepest descent reaction paths and can have turning points. However, steepest descent paths and gradient extremals coincide at stationary points and at points where the curvature of the steepest descent path is zero. Like steepest descent paths, gradient extremals depend on the coordinate system. Methods for following gradient extremal paths are outlined below; detailed discussions of the features of gradient extremals are available in the literature.[5]

2 STEEPEST DESCENT REACTION PATHS

To describe the steepest descent reaction path, the coordinates along the path, $\vec{x}(s)$ are written as a parametric function of the arc length along the path, s. The path can then be expanded in a Taylor series:

$$\vec{x}(s)=\vec{x}(s_0)+\vec{v}^0(s-s_0)+1/2\vec{v}^1(s-s_0)^2+1/6\vec{v}^2(s-s_0)^3\cdots \quad (1)$$

where $\vec{v}^0$ is the tangent and $\vec{v}^1$ is the curvature. For a steepest descent path, the tangent is parallel to the gradient or first derivatives:

$$\vec{v}^0(s)=\frac{d\vec{x}(s)}{ds}=-\frac{\vec{g}(s)}{|\vec{g}(s)|} \quad (2)$$

where $\vec{g}(s)$ is the gradient at $\vec{x}(s)$. At the transition structure, the gradient is zero, and the tangent is equal to the eigenvector of the Hessian (or second derivative matrix) with the negative eigenvalue. In mass-weighted coordinates, this corresponds to the normal mode of vibration with the imaginary frequency.

The curvature, $\vec{v}^1$, is the rate of change of the tangent, and can be written in terms of the Hessian, **H**:

$$\vec{v}^1=\frac{d\vec{v}^0}{ds}=\frac{d^2\vec{x}}{ds^2}=-\frac{(\mathbf{H}\vec{v}^0-(\vec{v}^{0t}\mathbf{H}\vec{v}^0)\vec{v}^0)}{|\vec{g}|} \quad (3)$$

The curvature vector indicates how sharply the reaction path bends, and points toward the inside of the bend. The magnitude of the curvature, κ, is equal to the inverse of the radius of curvature, $\kappa=|\vec{v}^1|=1/R$, i.e., large curvature corresponds to a tight bend with a small radius. At the transition structure (TS), both the numerator and the denominator of equation (3) are zero; however, the curvature can be found by applying l'Hospital's rule:

$$\vec{v}^1=-(\mathbf{H}-2(\vec{v}^{0t}\mathbf{H}\vec{v}^0)\mathbf{I})^{-1}(\mathbf{F}^1\vec{v}^0-(\vec{v}^{0t}\mathbf{F}^1\vec{v}^0)\vec{v}^0), \text{ at the TS} \quad (4)$$

where $F^1_{ij}=\sum_k F_{ijk}\vec{v}^0_k$ and F_{ijk} is the matrix of third derivatives. $\mathbf{F}^1\vec{v}^0$ can be calculated via numerical second differentiation of the gradient by displacing along the tangent.

Reaction path following methods yield a discrete set of points $\vec{x}_i$ along the path rather than a continuous function. These points can be found by starting at the transition structure and using numerical methods to solve equation (2), the differential equation that defines the steepest descent reaction path. A variety of numerical methods are available for solving ordinary differential equations (ODE) of one variable.[10] Methods for solving differential equations are usually classified by order, i.e., a second-order method gives the correct first and second-order terms of the Taylor expansion of the exact solution. Most techniques for integrating differential equations are explicit methods, in that the expression for the step does not involve the gradient at the end-point of the step. However, equation (2) is a stiff differential equation, and special care must be taken in solving it.[11] Implicit methods, i.e., ones that require the gradient at the end-point of the step, are stable for stiff differential equations whereas explicit methods may be less stable and require much smaller step sizes.

2.1 First-order Methods

The method of Ishida, Morokuma, and Komornicki[12] (IMK) is shown in Figure 3(a). It is a modification of the explicit Euler method that adds a stabilization step; hence it is also known as the Euler stabilization method (ES). An explicit Euler step of length σ is taken from $\vec{x}_i$ along the tangent $\vec{v}_i$ to a point $\vec{x}'_{i+1}=\vec{x}_i+\sigma\vec{v}^0_i=\vec{x}_i-\sigma\vec{g}_i/|\vec{g}_i|$. The energy and gradient are calculated at $\vec{x}'_{i+1}$. The stabilization step consists of minimizing the energy along the bisector of the angle between $-\vec{g}'_{i+1}$ and $\vec{x}_i-\vec{x}'_{i+1}$. The minimum along the bisector is taken

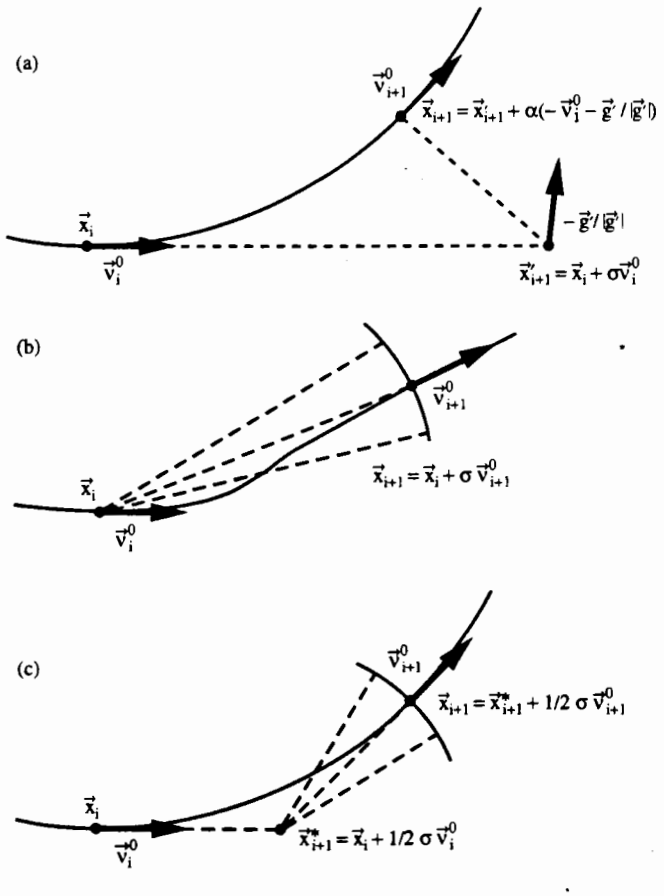

Figure 3 Reaction path following algorithms: (a) first-order method of Ishida, Morokuma, and Komornicki (IMK), (b) first-order method of Müller and Brown (MB), and (c) second-order method of Gonzalez and Schlegel (GS). Reproduced with permission from H. B. Schlegel, in 'Modern Electronic Structure Theory', ed. D. R. Yarkony. Copyright (1995) World Scientific Publishing

as the next point on the path, $\vec{x}_{i+1}$. For very small step sizes or angles close to 180°, the stabilization step must be omitted. In difficult regions of the potential energy surface, very small steps may be needed to prevent oscillations about the true path.

The Müller–Brown method (MB) (Figure 3b)[13] is an implicit Euler method. A step of length σ is taken from $\vec{x}_i$ and the energy is minimized under the constraint of constant step length, $|\vec{x}_{i+1} - \vec{x}_i| = \sigma$. At the minimum, the residual gradient is parallel to the step. Thus the implicit Euler step can also be written as $\vec{x}_{i+1} = \vec{x}_i - \sigma\vec{g}_{i+1}/|\vec{g}_{i+1}| = \vec{x}_i + \sigma\vec{v}^0_{i+1}$

2.2 Second-order Methods

Standard numerical methods such as second-order Runge-Kutta could be used, but a more effective approach is to expand the potential energy surface in equation (2) to second order and integrate the resulting expression from $\vec{x}_i$ to $\vec{x}_{i+1}$. This yields the local quadratic approximation (LQA) of Page and McIver[14] which is an explicit second-order method.

$$\frac{d\vec{x}}{ds} = -\frac{\vec{g}_i + \mathbf{H}_i(\vec{x} - \vec{x}_i)}{|\vec{g}_i + \mathbf{H}_i(\vec{x} - \vec{x}_i)|} \tag{5}$$

Sun and Ruedenberg obtained improved performance by using $\vec{x}_i$ as the midpoint of the integration range rather than the start.[16c] Page and McIver also developed the CLQA method, a correction to the LQA method involving a component of the third derivatives.[16a]

$$\vec{x}_{i+1,\mathrm{CLQA}} = \vec{x}_{i+1,\mathrm{LQA}} + 1/6\Delta\vec{v}^2\Delta s^3;$$
$$\Delta\vec{v}^2 = -(\mathbf{F}^1\vec{v}^0 - (\vec{v}^{0\alpha}\mathbf{F}^1\vec{v}^0)\vec{v}^0), /|\vec{g}| \tag{6}$$

Gonzalez and Schlegel[15] (GS) devised the second-order implicit method shown in Figure 3(c). A step of length 1/2 σ is taken from $\vec{x}_i$ to a pivot point, $\vec{x}^*_{i+1}$ (no calculation of E or $\vec{g}$ at $\vec{x}^*_{i+1}$). A step of length 1/2 σ is taken from the pivot point and the energy is minimized subject to $|\vec{x}_{i+1} - \vec{x}^*_{i+1}| =$ 1/2 σ, yielding the next point on the path, $\vec{x}_{i+1}$. The points $\vec{x}_i$, $\vec{x}^*_{i+1}$, and $\vec{x}_{i+1}$ form an isosceles triangle that is tangent to the path at $\vec{x}_i$ and $\vec{x}_{i+1}$ by construction. Since two tangents to a circle form an isosceles triangle, the reaction path between $\vec{x}_i$ and $\vec{x}_{i+1}$ can be represented by an arc of a circle. The total step can be written as

$$\vec{x}_{i+1,\mathrm{GS}} = \vec{x}_i + 1/2\sigma\vec{v}^0_i + 1/2\sigma\vec{v}^0_{i+1} \tag{7}$$

This approach is similar to the implicit trapezoid method for integrating stiff differential equations,[11] but uses an optimization to obtain the final point.

The LQA, CLQA, and GS methods yield the exact tangent and curvature vectors along the path in the limit of infinitesimal step size, whereas the first-order methods reproduce only the tangent. The GS and CLQA methods also give the correct curvature vector at the transition structure, but the LQA method does not.

2.3 Higher-order Methods

Fourth-order Runge-Kutta and various predictor–corrector methods have been used successfully for reaction path following, especially on analytical potential energy surfaces.[16] Page and McIver have extended the LQA and CLQA methods to a family of higher-order methods that employ first, second and higher derivatives of the potential energy surface.[14] Gonzalez and Schlegel developed a series of higher-order implicit methods for path following.[17] One of these employs the tangent and curvature at the beginning and end points of the step to obtain a fourth-order implicit method:

$$\vec{x}_{i+1,\mathrm{GS4}} = \vec{x}_i + 1/2\sigma\vec{v}^0_i + 1/2\sigma\vec{v}^0_{i+1} + 1/12\sigma^2\vec{v}^1_i - 1/12\sigma^2\vec{v}^1_{i+1} \tag{8}$$

2.4 Relaxation Methods

An alternate approach to finding a reaction path starts with a set of points on an approximate path and then refines or relaxes them until the appropriate conditions are met. Jasien and Shepard describe a method for fitting the potential energy surface around the reaction path.[18] They calculate energies and first and second derivatives at a number of points along a reference path and fit a polynomial spline surface to the data. The fitted surface is then used to improve the reference path, and the process is repeated until it converges to the steepest descent path. Elber and Karplus[19] refined the path by minimizing the integral of the energy along the path:

$$S = \frac{1}{L}\int_{\vec{x}_0}^{\vec{x}_N} E(\vec{x}(s))ds \approx \frac{1}{L}\sum_{i=1}^{N}\frac{E(\vec{x}_i) + E(\vec{x}_{i-1})}{2}|\vec{x}_i - \vec{x}_{i-1}| \tag{9}$$

This approach does not require the transition structure to be optimized first and will also find any intermediates along the reaction path if they exist. However, self-avoidance and equal spacing constraints are needed so that the path does not collapse into the minima, and these constraints cause the relaxation process to converge slowly. Stacho and Ban[20] describe a 'dynamically defined reaction path' (DDRP) procedure, in which an initial path is improved by taking a steepest descent step for each point and then redistributing the points to maintain equal spacing. After numerous iterations, this approach converges to the steepest descent path and will correctly handle multiple stationary points along the path. Ayala and Schlegel[21] refined the approximate path by optimizing the highest point to the transition structure and requiring the remaining points to satisfy the steepest descent reaction path equation. The number of steps is comparable to conventional methods for transition structure optimization and reaction path following.

2.5 Projected Frequencies and Coupling Matrix Elements

In order to use variational transition state theory or reaction path Hamiltonian methods (see ***Transition State Theory***) to calculate rate constants, one needs vibrational frequencies perpendicular to the reaction path. These are obtained by projecting out motion along the tangent, $\vec{v}^0$. The projector, $\mathbf{P}$, and the projected Hessian, $\tilde{\mathbf{H}}$, are given by

$$\mathbf{P} = \mathbf{I} - \vec{v}^0\vec{v}^{0\alpha}; \tilde{\mathbf{H}} = \mathbf{PHP} \tag{10}$$

The projected frequencies can then be calculated from the projected Hessian in the usual fashion.[22] If mass-weighted Cartesian coordinates are used, rigid body translation and rotation are also projected out. In addition to the projected frequencies, one also needs the coupling matrix elements, $\tilde{\mathbf{B}}$,

between motion along the path and the normal modes of vibration perpendicular to the path, $\vec{L}_i$.

$$\vec{B}_i = \vec{v}^{0t}\frac{d\vec{L}_i}{ds} = -\vec{v}^{1t}\vec{L}_i \tag{11}$$

The second equality can be obtained by differentiating $\vec{v}^{0t}\vec{L}_i = 0$ by s, and recalling $\vec{v}^1 = d\vec{v}^0/ds$. To obtain accurate projected frequencies and coupling matrix elements, the reaction path must be followed with a high degree of precision,[23] especially near the transition state where the gradient is small, and also in steep-sided valleys where small deviations from the true path can cause large errors in the tangent and curvature vectors.

2.6 Bifurcation and Valley-Ridge Inflection Points

A reaction path in a simple valley will have projected frequencies that are all real; equivalently all of the eigenvalues of the Hessian for motion perpendicular to the path are positive. If some of the frequencies are imaginary (or eigenvalues negative), the potential energy surface perpendicular to the path has a maximum. This indicates that the path is on a ridge rather than in a valley. The onset of the ridge is marked by a valley-ridge inflection (VRI) point, where a projected frequency is zero.[24] Algorithms have been developed for locating VRI points.[25]

The presence of a VRI point indicates that a simple valley branches or bifurcates into two valleys. A bifurcation can occur as a valley descends from a transition structure and splits into two valleys. It can also occur as a valley rises and branches to two transition structures. In potential energy surfaces with bifurcations, reaction paths computed in different coordinate systems may follow different valleys, depending on which side of the ridge they fall. Note, however, that a steepest descent reaction path passing through a VRI point will stay on the ridge until it reaches a stationary point, rather than bifurcating at the VRI point. As shown in Figure 1, even if the path is displaced sideways from the ridge, it will follow the ridge for quite a distance before descending into one of the valleys.

3 GRADIENT EXTREMALS

When a point is on a gradient extremal path, the gradient is an eigenvector of the Hessian.[5]

$$\mathbf{H}(\vec{x})\vec{g}(\vec{x}) = \lambda\vec{g}(\vec{x}) \tag{12}$$

If this relation is substituted into equations (2) and (3), it can be seen that the steepest descent path through any point on a gradient extremal has zero curvature. For a quadratic expansion of the energy about an arbitrary point on the potential surface, a step of $\Delta\vec{x}$ can be taken toward the gradient extremal path,

$$\Delta\vec{x} = \alpha\vec{u} - \mathbf{P}'\mathbf{H}^{-1}\vec{g};\mathbf{P}' = (\mathbf{I} - \vec{u}\vec{u}') \tag{13}$$

where $\vec{u}$ is the eigenvector of $\mathbf{H}$ that corresponds to the eigenvalue λ. The step consists of a displacement along the eigenvector and a Newton-Raphson minimization step in the space perpendicular to the path.[26] In practice, the total step length is adjusted so that it does not exceed a trust radius. It is possible to avoid calculating the Hessian at each step by using a suitable updating scheme.[27]

The condition for being on the gradient extremal path, equation (13), can also be written as:

$$\mathbf{PH}\vec{g} = \vec{0};\mathbf{P} = \mathbf{I} - \vec{v}^0\vec{v}^{0t};\vec{v}^0 = -\vec{g}/|\vec{g}| \tag{14}$$

Equation (14) can be used to search for the gradient extremal path directly by stepping along the path and solving for $\mathbf{P}\,\mathbf{H}\,\vec{g} = \vec{0}$ or minimizing $(\mathbf{P}\,\mathbf{H}\,\vec{g})^2$; numerical differentiation can be used to compute $\mathbf{H}\,\vec{g} \approx (\vec{g}(\vec{x} + h\vec{g}) - \vec{g}(\vec{x}))/h$, thus avoiding the calculation of the full Hessian.[27,28]

Equation (14) can be expanded in the neighborhood of $\vec{x}_0$:

$$\mathbf{PH}\vec{g} + \nabla(\mathbf{PH}\vec{g})(\vec{x} - \vec{x}_0) + \cdots = \vec{0} \tag{15}$$

$$\nabla(\mathbf{PH}\vec{g}) = \mathbf{P}(\mathbf{F} + \mathbf{H}^2 - (\vec{v}^{0t}\mathbf{H}\vec{v}^0)\mathbf{H}) - \vec{v}^0\vec{v}^{0t}(\mathbf{H}^2 - (\vec{v}^{0t}\mathbf{H}\vec{v}^0)\mathbf{H}) \tag{16}$$

where $F_{ij} = \sum_k F_{ijk}\vec{g}_k$ and F_{ijk} is the matrix of third derivatives. If the gradient extremal path is also expanded about a point on the path, $\vec{x} = \vec{x}_0 + \vec{v}(s - s_0) + \cdots$ and substituted into equation (15), then $\vec{v}$, the tangent to the gradient extremal path, can be obtained by solving:[28]

$$\nabla(\mathbf{PH}\vec{g})\vec{v} = \vec{0};\nabla(\mathbf{PH}\vec{g}) = \mathbf{PF} + \mathbf{H}^2 - \lambda\mathbf{H} \quad \text{on the gradient extremal path} \tag{17}$$

Note that, if the third derivative term is not zero, then the tangent to the gradient extremal is not an eigenvector of $\mathbf{H}$. Instead of stepping along the eigenvector, $\vec{u}$, an improved method for following the gradient extremal path described by Sun and Ruedenberg[28] steps along $\vec{v}$, the correct tangent, so that $\vec{x}'_{i+1} = \vec{x}_i + \sigma\vec{v}_i$. The gradient and Hessian are calculated at $\vec{x}_{i+1}$, and equations (15) and (16) can be used to calculate a correction step,

$$\vec{x}_{i+1} = \vec{x}'_{i+1} - \mathbf{A}[\mathbf{A}\mathbf{A}']^{-1}(\mathbf{PH}\vec{g}) \tag{18}$$

where $\mathbf{P}\,\mathbf{H}\,\vec{g}$ and $\mathbf{A} = \mathbf{P}\nabla(\mathbf{PH}\vec{g})$ are computed at $\vec{x}'_{i+1}$ and a generalized inverse is used.

A bifurcation in a gradient extremal path occurs when there is more than one independent solution to equation (16). Appropriate cautions are need to follow a gradient extremal through bifurcations.[29] Unlike steepest descent paths, gradient extremals can also have turning points where an uphill path changes to a downhill path or vice versa. These are characterized by a tangent perpendicular to the gradient, and can occur near cirques and cliffs on potential energy surfaces. While steepest descent reaction paths generally simplify the description of potential energy surfaces, the multitude of bifurcations and turning points encountered with gradient extremals can lead to complicated topology even for small systems such as H_2CO.[29]

4 RELATED ARTICLES

Reaction Path Hamiltonian and its Use for Investigating Reaction Mechanisms; Scaled Particle Theory; Trajectory Simulations of Molecular Collisions: Classical Treatment; Transition State Theory.

5 REFERENCES

1. D. Heidrich, W. Kliesch, and W. Quapp, 'Properties of Chemically Interesting Potential Energy Surfaces', Springer-Verlag, Berlin, 1991; D. Heidrich (ed.), 'The Reaction Path in Chemistry: Current Approaches and Perspectives', Kluwer, Dordrecht, 1995.
2. M. L. McKee and M. Page, *Rev. Comput. Chem.*, 1993, **4**, 35-65.
3. H. B. Schlegel, in 'Modern Electronic Structure Theory', ed. D. R. Yarkony, World Scientific Publishing, 1995, pp. 459-500.
4. M. A. Collins, *Adv. Chem. Phys.*, 1996, **93**, 389-453.
5. J. Pancir, *Coll. Czech. Chem. Commun.*, 1975, **40**, 1112-1118; M. V. Basilevsky and A. G. Shamov, *Chem. Phys.*, 1981, **60**, 347-358; D. K. Hoffman, R. S. Nord, and K. Ruedenberg, *Theor. Chim. Acta*, 1986, **69**, 265-279.
6. K. Fukui, *Acc. Chem. Res.*, 1981, **14**, 363-368.
7. W. Quapp and D. Heidrich, *Theor. Chim. Acta*, 1984, **66**, 245-260.
8. J. J. P. Stewart, L. P. Davis, and L. W. Burggraf, *J. Comput. Chem.*, 1987, **8**, 1117-1123; S. A. Maluendes and M. J. Dupuis, *J. Chem. Phys.*, 1990, **93**, 5902-5911; M. S. Gordon, G. Chaban, and T. Taketsugu, *J. Phys. Chem.*, 1996, **100**, 11512-11525.
9. K. Bolton, W. L. Hase, and G. H. Peslherbe, in 'Modern Methods in Multidimensional Dynamics Computations in Chemistry', ed. D. L. Thompson, World Scientific Publishing, 1998.
10. W. H. Press, B. P. Flannery, S. A. Teukolsky, and W. T. Vetterling, 'Numerical Recipes', Cambridge University Press, 1989.
11. C. W. Gear, 'Numerical Initial Value Problems in Ordinary Differential Equations', Prentice-Hall, 1971.
12. K. Ishida, K. Morokuma, and A. Komornicki, *J. Chem. Phys.*, 1977, **66**, 2153-2156; M. W. Schmidt, M. S. Gordon, and M. Dupuis, *J. Am. Chem. Soc.*, 1985, **107**, 2585-2589.
13. K. Müller and L. D. Brown, *Theor. Chim. Acta*, 1979, **53**, 75-93.
14. (a) M. Page and J. W. McIver, Jr., *J. Chem. Phys.*, 1988, **88**, 922-935; (b) M. Page, C. Doubleday, and J. W. McIver, Jr., *J. Chem. Phys.*, 1990, **93**, 5634-5642; (c) J. Q.-Sun and K. Ruedenberg, *J. Chem. Phys.*, 1993, **99**, 5269-5275.
15. C. Gonzalez and H. B. Schlegel, *J. Chem. Phys.*, 1989, **90**, 2154-2161; *J. Phys. Chem.*, 1990, **94**, 5523-5527.
16. K. K. Baldridge, M. S. Gordon, R. Steckler, and D. G. Truhlar, *J. Phys. Chem.*, 1989, **93**, 5107-5119; V. S. Melissas, D. G. Truhlar, and B. C. Garrett, *J. Chem. Phys.*, 1992, **96**, 5758-5772.
17. C. Gonzalez and H. B. Schlegel, *J. Chem. Phys.*, 1991, **95**, 5853-5860.
18. P. G. Jasien and R. Shepard, *Int. J. Quantum Chem., Quantum Chem. Symp.*, 1988, **22**, 183-198.
19. R. Elber and M. Karplus, *Chem. Phys. Lett.*, 1987, **139**, 375-380.
20. L. L. Sacho and M. I. Bán, *Theor. Chim. Acta*, 1992, **83**, 433-440.
21. P. Ayala and H. B. Schlegel, *J. Chem. Phys.*, 1997, **107**, 375-384.
22. E. B. Wilson, J. C. Decius, and P. C. Cross, 'Molecular Vibrations', McGraw-Hill, New York, 1955.
23. A. G. Basoul and H. B. Schlegel, *J. Chem. Phys.*, 1997, **107**, 9413-9417.
24. P. Valtazanos and K. Ruedenberg, *Theor. Chim. Acta*, 1986, **69**, 281-307.
25. J. Baker and P. M. W. Gill, *J. Comput. Chem.*, 1988, **9**, 465-475.
26. P. Jørgensen, H. J. Jensen, and T. Helgaker, *Theor. Chim. Acta*, 1988, **73**, 55-65.
27. H. B. Schlegel, *Theor. Chim. Acta*, 1992, **83**, 15-20.
28. J. Q.-Sun and K. Ruedenberg, *J. Chem. Phys.*, 1993, **98**, 9707-9714.
29. K. Bondensgard and F. Jensen, *J. Chem. Phys.*, 1996, **104**, 8025-8031.

Reaction Path Hamiltonian

See *Reaction Path Following*.

Reaction Path Hamiltonian and its Use for Investigating Reaction Mechanisms

Elfi Kraka

Göteborg University, Sweden

Abbreviations

LAM = large amplitude motion; RP = reaction path; RPH = reaction path Hamiltonian; RSH = reaction surface Hamiltonian; SAM = small amplitude motion; SRP = specific reaction parameter; SRPH = solution reaction path Hamiltonian.

1 INTRODUCTION

Key issues in chemistry are the description and understanding of mechanism and dynamics of chemical reactions. In principle, this understanding can be obtained by designing and carrying out suitable experiments. However, in practice it is rather difficult to get a detailed mechanistic and dynamic description of even the simplest chemical reactions. This has to do with the fact that apart from reactants, products, and possible stable intermediates, all other molecular forms encountered during a reaction have such a short lifetime that standard experimental means are not sufficient to detect and describe them. Progress in modern laser spectroscopy seems to provide an access to transient species with lifetimes in the pico- to femtosecond region;[1] however, much more development in this research area is needed to make this approach a standard experimental method for describing reaction mechanism and reaction dynamics in detail.

Today, computational investigations utilizing state-of-the art methods of quantum chemistry, in particular *ab initio* methods, provide the major source of knowledge on reaction mechanism and reaction dynamics. For this purpose, the interactions between the atomic and/or molecular species involved in a reaction are calculated and analyzed with the help of *ab initio* methods.